

Quasi-one-dimensional Spin Dynamics in a Molecular Spin Liquid System

Yugo Oshima,^{1,*} Yasuyuki Ishii,² Francis L. Pratt,³ Isao Watanabe,⁴
Hitoshi Seo,^{1,5} Takao Tsumuraya,⁶ Tsuyoshi Miyazaki,⁷ and Reizo Kato¹

¹RIKEN Cluster for Pioneering Research, Wako, Saitama 351-0198, Japan.

²College of Engineering, Shibaura Institute of Technology, Minuma-ku, Saitama 337-8570, Japan.

³ISIS Neutron and Muon Source, STFC Rutherford Appleton Laboratory, Chilton, Oxfordshire OX11 0QX, UK

⁴RIKEN Nishina Center, Wako, Saitama 351-0198, Japan.

⁵RIKEN Center for Emergence Matter Science (CEMS), 2-1 Hirosawa, Wako, Saitama 351-0198, Japan.

⁶Magnesium Research Center, Kumamoto University, Kumamoto 860-8555, Japan

⁷Research Center for Materials Nanoarchitectonics (MANA),

National Institute for Materials Science, Tsukuba, Ibaraki 305-0044, Japan

(Dated: October 29, 2024)

The molecular triangular lattice system, β' -EtMe₃Sb[Pd(dmit)₂]₂, is considered as a candidate material for the quantum spin liquid (QSL) state, although ongoing debates arise from recent controversial results. Here, the results of electron spin resonance (ESR) and muon spin relaxation (μ SR) measurements on β' -EtMe₃Sb[Pd(dmit)₂]₂ are presented. Both results indicate characteristic behaviors related to quasi-one-dimensional (q1D) spin dynamics, whereas the direction of anisotropy found in ESR is in contradiction with previous theories. We succeed in interpreting the experiments by combining density-functional theory calculations and analysis of the effective model taking into account the multi-orbital nature of the system. While the QSL-like origin of β' -EtMe₃Sb[Pd(dmit)₂]₂ was initially attributed to the magnetic frustration of the triangular lattice, it appears that the primary origin is a 1D spin liquid resulting from the dimensional reduction effect.

Ground states of magnetically frustrated triangular lattice systems, where antiferromagnetically coupled $S=1/2$ spins are positioned on each lattice site, have posed a long-standing challenge in condensed matter physics since Anderson proposed the resonating-valence-bond (RVB) state for the $S=1/2$ Heisenberg model on a uniform triangular lattice [1–7]. Although confirmation of the quantum spin liquid (QSL) state has remained elusive, several molecular materials with $S=1/2$ triangular lattices have garnered significant attention [8–15]. One notable QSL candidate is the dimer-Mott insulator β' -EtMe₃Sb[Pd(dmit)₂]₂, where dmit, Et and Me are 1,3-dithiole-2-thione-4,5-dithiolate, ethyl and methyl, respectively [13–16].

β' -EtMe₃Sb[Pd(dmit)₂]₂ consists of Pd(dmit)₂ anions and a monovalent counteranion EtMe₃Sb⁺. The anions form strongly dimerized [Pd(dmit)₂]₂⁻, and an electron is localized on each dimer. As shown in Fig. 1, the crystal structure of β' -EtMe₃Sb[Pd(dmit)₂]₂ has two crystallographically equivalent Pd(dmit)₂ layers with different dimer stacking direction (layer A and B). Layers A and B are connected by the glide plane symmetry. The Pd(dmit)₂ dimers form a $S=1/2$ triangular lattice on each layer, where the transfer integral along the dimer's stacking direction is denoted as t_B , the side-by-side direction as t_S , and the diagonal direction as t_r (Fig. 1). The calculated transfer integrals between the dimers suggest a nearly isosceles or scalene triangular arrangement in the magnetic geometry (see Table I) [17–22]. β' -EtMe₃Sb[Pd(dmit)₂]₂ shows no magnetic long-range order down to approximately 40 mK, which is several orders of magnitude lower than its exchange interaction [23–33]. Precise tuning of the transfer integrals using mixed coun-

tercations further reveals the presence of a QSL ‘phase’ in the system [34].

However, the nature of its QSL-like ground state is so far controversial. The specific heat and the first report of thermal conductivity measurements both show linear temperature dependence, although it is an insulator [24, 25]. Such behavior is considered to be originating from the delocalized nature of the excitations and it was proposed to be owing to the existence of spinons with a Fermi surface. However, theoretical studies for a QSL state with a spinon Fermi surface find $T^{2/3}$ scaling rather than linear scaling [35]. Furthermore, in contradiction to the initial study of thermal conductivity, recent studies performed by three different groups report the absence of any residual linear term κ_0/T [29, 30, 33], while Yamashita *et al.* have reported that the linear term depends on the sample and in particular the cooling rate [31, 32, 36]. No cooling rate dependence is observed in X-ray diffraction, transport and NMR, though [37]. As for alternative ground states, several competing charge-order states are proposed through vibrational spectroscopy [28]. A random-singlet state due to random intradimer charge disproportionation is proposed since a relaxor-type ferroelectricity was observed [38–40]. Moreover, a recent *ab-initio* calculation proposed that the QSL state of β' -EtMe₃Sb[Pd(dmit)₂]₂ is essentially a 1D spin-liquid, although it preserves some two-dimensionality [22].

In this Letter, we present a different experimental approach for studying the ground state of β' -EtMe₃Sb[Pd(dmit)₂]₂ using electron spin resonance (ESR) and muon spin rotation (μ SR). Both results exhibit characteristic features of a quasi-one-dimensional

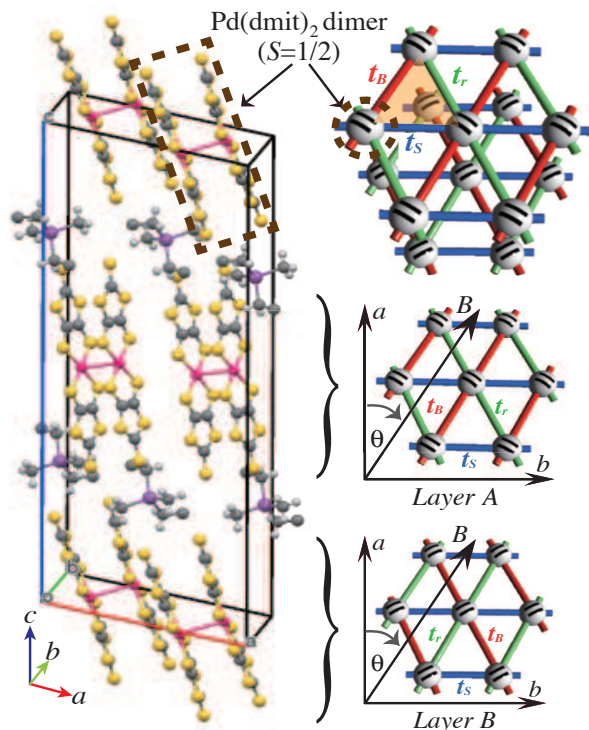


FIG. 1. (left) Crystal structure of β' -EtMe₃Sb[Pd(dmit)₂]₂. Two crystallographically equivalent Pd(dmit)₂ layers with different dimer stacking directions exist in the unit cell (Layer A and B), and the Pd(dmit)₂ dimer with $S=1/2$ forms a triangular lattice in each layer. (right) Schematic drawings of the triangular lattice and its transfer integrals for layers A and B. θ is the angle of the magnetic field from the a -axis used for ESR.

TABLE I. Interdimer transfer integrals (in meV) along the three directions of the triangular lattice of β' -EtMe₃Sb[Pd(dmit)₂]₂ evaluated by different methods. The low-temperature crystal structure data has been used for our calculation. FP, TB and EHM stands for first-principles calculation, tight-binding and extended Hubbard models, respectively. The number of bands included in the analysis is indicated.

Methods	t_B	t_S	t_r	Ref.
Extended Hückel	34	33	26	[17]
FP + TB (6-band)	54	45	40	[18]
FP + TB (2-band)	49	45	37	[19]
FP + TB (2-band)	55	47	39	[20]
FP + TB (2-band)	57	45	40	[21]
FP + TB (2-band)	57	45	40	[22]
FP + TB (8-band) + EHM	31	28	36	present study

(q1D) spin dynamics, with the fastest propagation direction for spin dynamics being along t_r , which corresponds to the direction of weakest magnetic coupling, as indicated by previous calculations [17–22]. By extending the theoretical analysis to include the multi-orbital nature of the system, we show a renewed picture of the magnetic

anisotropy, finding good agreement with the experimental results. Our finding suggests the QSL ground state of β' -EtMe₃Sb[Pd(dmit)₂]₂ is another example of ‘dimensional reduction’ induced by frustration and quantum fluctuations.

Single crystals of β' -EtMe₃Sb[Pd(dmit)₂]₂ were prepared using the method described in Ref. [30]. ESR measurements were carried out with a conventional X-band ESR spectrometer (~ 9.1 GHz), using a single crystal (approximately $1 \times 1 \times 0.05$ mm³) mounted on a quartz rod to allow rotation in the ab -plane. The μ SR experiments were performed at the RIKEN-RAL muon facility in the UK and the S μ S facility in Switzerland. Randomly oriented crystals, with a total weight of 100 mg, were wrapped in a packet of 12.5 μ m silver foil and attached to the sample plate of a helium dilution refrigerator. Further details of the experimental setups and theoretical calculations can be found in the Supporting Information (SI) [41].

Two distinct ESR signals are observed when the magnetic field is rotated within the ab -plane of the triangular lattice of the β' -EtMe₃Sb[Pd(dmit)₂]₂ salt. The observed ESR spectra are presented in Fig. S2 [41]. The angular dependence of the g -values, obtained from the ESR signals, shows two almost identical components of the g -tensor with a shift between them of about 30° (Fig. 2(a)). This g -tensor shift coincides with the difference in the stacking direction of the Pd(dmit)₂ dimers between adjacent layers, as shown in Fig. 1. Hence, the principal axes of the g -tensor are related to the orientation of the Pd(dmit)₂ dimers ($S=1/2$), and the minimum and the maximum of the g -value are observed when the magnetic field is respectively applied parallel and perpendicular to the stacking direction of the Pd(dmit)₂ dimers. The perpendicular direction is close to the b -axis side-by-side direction of the dimer arrangement. From the comparison of the g -values with the crystal axes, the two ESR signals can be assigned to layer A and layer B of the Pd(dmit)₂ layers, shown as open and solid red circles in Fig. 2(a), respectively. These results show that the ESR origin is purely from the spins on the triangular lattice, and extrinsic effects from impurities are ruled out.

It is well known that if a finite exchange interaction exists between two spins with different g -tensors, the two independent ESR absorption lines merge into a single absorption line in a process known as exchange narrowing [42, 43]. The exchange interaction J can be roughly estimated from the relation $2J \sim |\Delta g| \mu_B B$, where Δg is the difference in the g -values when the amalgamation of ESR lines occurs. [42, 44] From Fig. 2(a), we observe that the amalgamation occurs where $\Delta g = 0.005$, leading to an estimated interlayer exchange interaction of approximately 0.54 mK. This small interlayer interaction suggests that the magnetic network of β' -EtMe₃Sb[Pd(dmit)₂]₂ is highly 2D, which is consis-

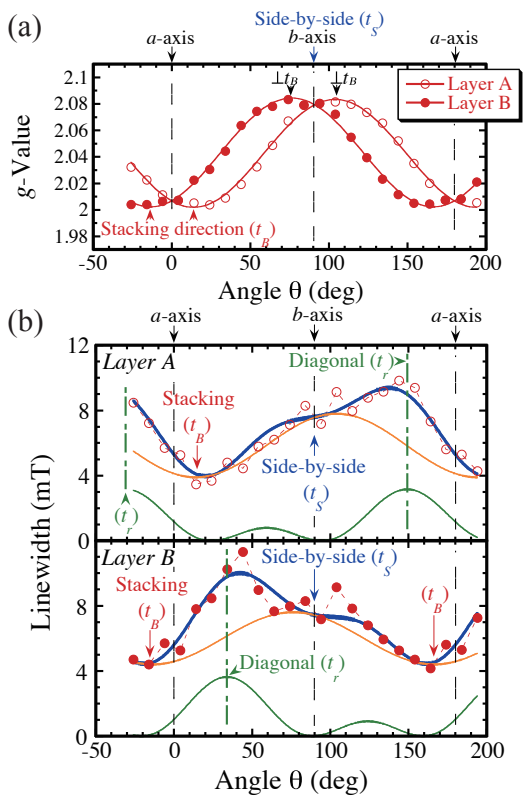


FIG. 2. The angular dependence of (a) the g -value and (b) the ESR linewidth of β' -EtMe₃Sb[Pd(dmit)₂]₂ at 4.7 K where the magnetic field is rotated within the ab -plane (a -axis is at $\theta=0^\circ$). Two ESR signals from layers A and B are presented as red open and solid circles, respectively. The angular dependence of the linewidth is fitted with the sum (thick blue curve) of $1 + \cos^2(\theta - \theta_{g\max})$ and $(3 \cos^2(\theta - \theta_{q1D}) - 1)^2$ terms, presented as orange and green solid curves, respectively. $\theta_{g\max}$ is 104° and 76° for layers A and B, respectively, which is in good agreement with the angle dependence of the g -tensors. θ_{q1D} is found to be 149° and 34° for layers A and B, respectively, which approximately corresponds to the diagonal direction t_r of the triangular lattice in each layer.

tent with the absence of long-range magnetic order in this system.

The in-plane angular dependence of the ESR linewidth at 4.7 K obtained from ESR of layers A and B are presented, respectively, as open and solid circles in Fig. 2(b). The linewidth shows an unconventional angular dependence, not previously seen in the case of a low-dimensional system or an inorganic triangular lattice [43, 45]. We find that this unusual angular dependence is well-fitted by a sum of $(1 + \cos^2 \theta)$ and $(3 \cos^2 \theta - 1)^2$ terms, which are presented respectively as orange and green solid curves in Fig. 2(b). The former angular dependence is a typical one for angle-dependent ESR and originates from the contributions of magnetic anisotropies to the g -values and dipolar or hyperfine interactions. For each layer, the extrema of the $(1 + \cos^2 \theta)$

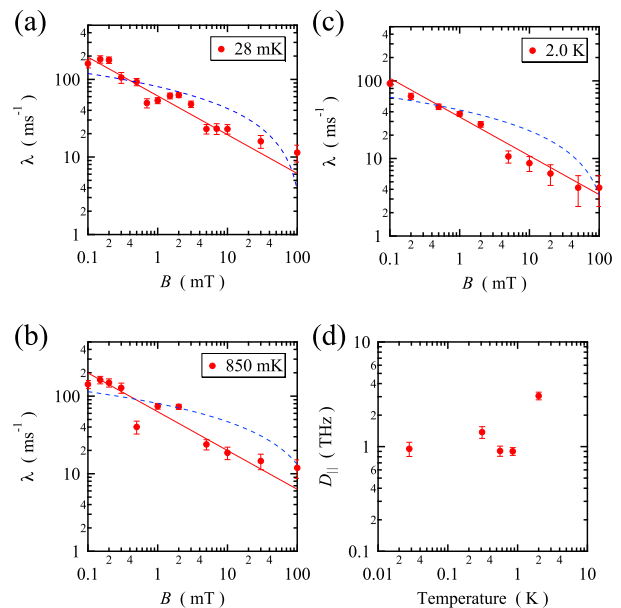


FIG. 3. Magnetic field dependence of the relaxation rate λ of β' -EtMe₃Sb[Pd(dmit)₂]₂ at (a) 28 mK, (b) 0.85 K, and (c) 2.0 K. The red solid lines and the blue dashed lines are the best fits from the q1D model and the 2D diffusive model, respectively. (d) Temperature dependence of intra-chain diffusion rate D_{\parallel} .

term coincide with those of the g -values (t_B and $\perp t_B$, respectively). The $(3 \cos^2 \theta - 1)^2$ angular term originates from q1D spin diffusion, which is commonly observed in ESR studies of low dimensional spin systems [43, 46–49]. For q1D spin diffusion, the direction showing the maximum of the linewidth corresponds to the diffusion direction. Our results show that the diffusive direction is along the diagonal direction of the triangular lattice (t_r) for both layers A and B. Despite our system consisting of a 2D triangular magnetic network, the ESR results indicate a q1D spin dynamics along t_r .

Next, we present our μ SR results for β' -EtMe₃Sb[Pd(dmit)₂]₂. Neither a spontaneous precession signal nor a divergence of the muon depolarization rate λ was observed down to low temperatures under zero-field conditions (ZF- μ SR, Fig. S3(a) in SI) [41]. These results show that there is no sign of long-range order down to 28 mK, in good agreement with the specific heat and thermal conductivity measurements [24, 25, 29–32]. Moreover, no excitation gap is found from the field dependence of the transverse-field muon spin rotation (TF- μ SR) measurements (Fig. S4).

To gain information from the spin dynamics, the field dependence of λ has been studied. Longitudinal-fields were applied along the muon-spin polarization direction (LF- μ SR) and the field-dependent muon-spin depolarization rate $\lambda(B)$ was measured at various temperatures (Figs. 3(a)-(c)). Each one shows a $B^{-0.5}$ dependence

over a wide field range of $0.1 < B < 100$ mT (red line in Figs. 3(a)-(c)) at temperatures below 2 K. This characteristic behavior reflects a 1D spin diffusion, which is fully in accordance with the ESR results. Note that our results cannot be fitted with a 2D diffusive model (blue dashed lines). From these field dependences, we could obtain diffusion rates D_{\parallel} using the expression

$$\lambda(B) = \frac{A^2}{4} (2D_{\parallel} \gamma_e B)^{-1/2} \quad (1)$$

where A is a scalar hyperfine coupling constant and γ_e is a gyromagnetic ratio of electron. Its derivation can be found in the SI [41]. Our DFT calculations for muon additions to $\text{Pd}(\text{dmit})_2$ using Gaussian16 [50] show the lowest energy when the muons were added to the end S site of $\text{Pd}(\text{dmit})_2$ molecule, with the corresponding experimental value of 71 MHz for A [41]. This value is comparable with the value of 82 MHz found for muonium addition at the end of the electron acceptor molecule TCNQ [51]. Using the obtained coupling constant, the diffusion rate D_{\parallel} is estimated as being of the order of 10^{12} s^{-1} . The temperature dependence of D_{\parallel} is shown in Fig. 3(d). We can also evaluate the degree of one-dimensionality from the data, giving a lower limit estimate of the ratio of intra-chain to inter-chain diffusion rate as $D_{\parallel}/D_{\perp} > 10^4$ [41]. This implies that the diffusion is highly 1D despite the three transfer integrals around the triangular unit having rather similar values, according to calculation.

The μSR and ESR results reveals a gapless ground state with a q1D spin dynamics. This might suggest the QSL-like ground state of β' - $\text{EtMe}_3\text{Sb}[\text{Pd}(\text{dmit})_2]_2$ is essentially a 1D spin-liquid. However, the diffusive direction is found to be along t_r , which is the smallest transfer integral from previous theoretical estimations as shown in Table I [17–22].

Following these results, we have reanalyzed its electronic structure (see Ref. [41] for details). Using first-principles calculations based on the density functional theory (DFT), we derive the maximally-localized Wannier functions (MLWFs) from 8 bands near the Fermi level. Here, following recent studies [21, 53], plane-wave DFT calculation within the generalized gradient approximation [54] was performed with the QUANTUM ESPRESSO code [55] using norm-conserving pseudopotentials [56, 57]. MLWFs were generated using the Wannier90 package [58, 59], by setting a Wannier center at each dmit ligand. Note that these MLWFs form not only the highest occupied molecular orbital (HOMO) but also the lowest occupied molecular orbital (LUMO), and eight bands are formed from them since there are four $\text{Pd}(\text{dmit})_2$ molecules in the unit cell. In Fig. 4(a), the DFT band structure is shown together with the tight-binding (TB) bands based on the MLWFs, whose spatial forms are shown in Fig. 4(b). The MLWFs are distributed on either side of the molecule, that show similarity to the wave functions introduced and called fragment

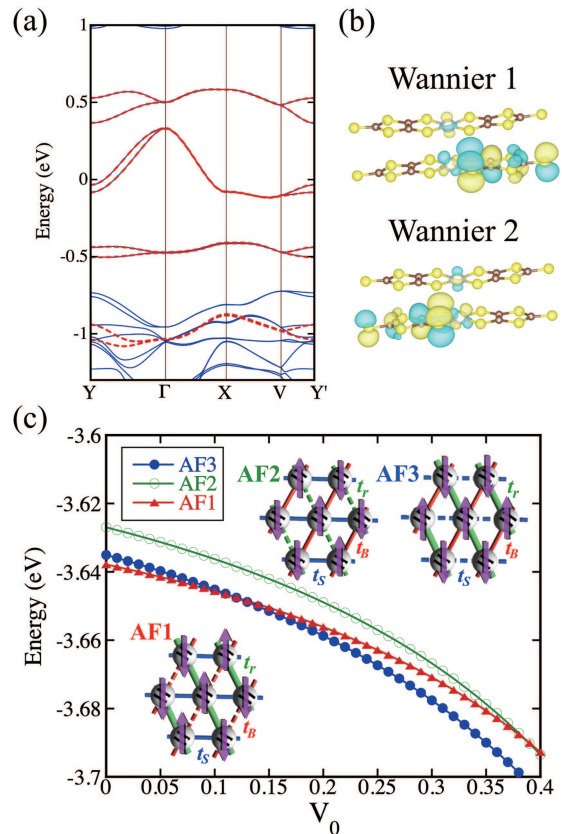


FIG. 4. (a) Band structure of β' - $\text{EtMe}_3\text{Sb}[\text{Pd}(\text{dmit})_2]_2$ (blue solid curves), and the TB bands based on the MLWFs (red broken curves). (b) Two independent MLWFs in the $\text{Pd}(\text{dmit})_2$ dimer, drawn using VESTA [52]. (c) Mean-field energies of different AF patterns varying the intersite Coulomb energies scaled by V_0 . The onsite Coulomb repulsion is set to $U=1.0$ eV. The AF alignments for each stable pattern are shown in the inset.

molecular orbital (fMO) in Ref. [60].

Based on the derived TB parameters, we investigate the electron correlation effect by the extended Hubbard model and compare the mean-field energies of different antiferromagnetic (AF) patterns. Fig. 4(c) shows the result for onsite Coulomb repulsion $U = 1.0$ eV, and varying the intersite Coulomb energies scaled by V_0 . One can see that AF1 and AF3 states are competing in energy, in which both patterns are AF along the t_r direction. This suggests that this direction indeed shows the strongest magnetic interaction.

We can evaluate the effective interdimer transfer integrals based on these calculations, following Ref. [60]. The wave function where $S = 1/2$ is localized is described by the linear combination of the fMOs, and their weights can be adopted from the mean-field solution which is about 1:3 within the molecule, consistent with the NMR measurement [61]. Typical parameters result in the values listed in Table I: Intriguingly, t_r becomes the largest. This difference from previous studies comes

from the multi-orbital nature; most studies have focused on the half-filled valence bands based on HOMO. However, the HOMO-LUMO levels in the isolated Pd(dmit)₂ molecule are close in energy with a separation of about 0.5 eV, while the Coulomb energy is of the same order [17, 20, 22, 62]. It is then natural to consider the multiple orbitals, and we have shown its significance in this study.

The competition and the fluctuation of the AF1 and AF3 states might suggest that the dimensional reduction effect takes place in the frustrated triangular lattice. In a similar manner to the triangular lattice system Cs₂CuCl₄, the magnetic frustration significantly reduces the interchain correlations in the ground state, and 1D physics similar to the spin-chain system can appear [3, 63–65]. Therefore, we conclude that the ground state of β'-EtMe₃Sb[Pd(dmit)₂]₂ might be a 1D spin liquid rather than a 2D QSL state of the triangular lattice.

Cs₂CuCl₄ exhibits dimensional reduction within an isosceles triangular magnetic lattice where $J'/J \sim 0.4$, and a small interlayer coupling stabilizes the 3D magnetic order below $T_N=0.6$ K [3, 63–65]. In contrast, β'-EtMe₃Sb[Pd(dmit)₂]₂ shows dimensional reduction even with the larger ratio $J'/J \sim 0.7$ (from the ratio of t^2 values), without any sign of long-range order. Such significant dimensional reduction and the lack of long-range order cannot be explained by a simple $S=1/2$ Heisenberg model, and other factors, such as charge and orbital degrees of freedom and the infinitesimal interlayer interaction, which causes AF instability, should be taken into account. Let us note that the range of J'/J where dimensional reduction and gapless excitation are theoretically observed remains controversial. For example, RVB type theories suggest $0 \leq J'/J \leq 0.25$ in Ref. [66] and $0 \leq J'/J \leq 0.65$ in Ref. [67]; the latter may give the upper bound. Further development of such theoretical approach might be able to account for the dimensional reduction we observe at the larger value of $J'/J \sim 0.7$. It is possible that the cation's orientational disorder in β'-EtMe₃Sb[Pd(dmit)₂]₂ also contributes to the AF instability [16]. However, the cation disorder does not seem to affect the magnetic network, as the diffusion anisotropy ratio remains highly 1D ($D_{\parallel}/D_{\perp} > 10^4$). Experimentally, the absence of long-range magnetic order in this system appears to be primarily determined by the infinitesimal interlayer interactions.

Muon site calculations were carried out using the STFC SCARF compute cluster. Part of this work was carried out at the ISIS Neutron and Muon Source, STFC Rutherford Appleton Laboratory, U.K. This work was partially supported by JSPS KAKENHI Grant Numbers JP20H04463 (IW), 23H01129 (HS), 23H04047 (HS), 23K03333 (HS).

* yugo@riken.jp

- [1] P. W. Anderson, Mater. Res. Bull. **8**, 153 (1973).
- [2] P. A. Lee, Science **321**, 1306 (2008).
- [3] L. Balents, Nature **464**, 199 (2010).
- [4] C. Lacroix, P. Mendels, and F. Mila, (Eds.) *Introduction to frustrated magnetism: Materials, Experiments, Theory*, Springer series in solid-state sciences (Springer, Berlin, 2011).
- [5] H. T. Diep, *Frustrated Spin System 2nd Edition* (World Scientific, 2013).
- [6] L. Savary and L. Balents, Rep. Prog. Phys. **80**, 016502 (2016).
- [7] Y. Zhou, K. Kanoda, and T. K. Ng, Rev. Mod. Phys. **89**, 025003 (2017).
- [8] Y. Shimizu, K. Miyagawa, K. Kanoda, M. Maesato, and G. Saito, Phys. Rev. B **73**, 140407(R) (2006).
- [9] S. Yamashita, Y. Nakazawa, M. Oguni, Y. Oshima, H. Nojiri, Y. Shimizu, K. Miyagawa, and K. Kanoda, Nat. Phys. **4**, 459 (2008).
- [10] M. Yamashita, N. Nakata, Y. Kasahara, T. Sasaki, N. Yoneyama, N. Kobayashi, S. Fujimoto, T. Shibauchi, and Y. Matsuda, Nat. Phys. **5**, 44 (2009).
- [11] F. L. Pratt, P. J. Baker, S. J. Blundell, T. Lancaster, S. Ohira-Kawamura, C. Baines, Y. Shimizu, K. Kanoda, I. Watanabe, and G. Saito, Nature **471**, 612 (2011).
- [12] T. Isono, H. Kamo, A. Ueda, K. Takahashi, M. Kimata, H. Tajima, S. Tsuchiya, T. Terashima, S. Uji, and H. Mori, Phys. Rev. Lett. **112**, 177201 (2014).
- [13] T. Itou, A. Oyamada, S. Maegawa, M. Tamura, and R. Kato, Phys. Rev. B **77**, 104413 (2008).
- [14] M. Tamura and R. Kato, Sci. Technol. Adv. Mater. **10**, 024304 (2009).
- [15] K. Kanoda and R. Kato, Annu. Rev. Condens. Matter Phys. **2**, 167 (2011).
- [16] R. Kato, Bull. Chem. Soc. Jpn. **87**, 355 (2014).
- [17] K. Ueda, T. Tsumuraya, and R. Kato, Crystals **8**, 138 (2018).
- [18] K. Nakamura, Y. Yoshimoto, and M. Imada, Physical Review B **86**, 205117 (2012).
- [19] E. P. Scriven and B. J. Powell, Phys Rev Lett **109**, 097206 (2012).
- [20] T. Tsumuraya, H. Seo, M. Tsuchiizu, R. Kato, and T. Miyazaki, J. Phys. Soc. Jpn. **82**, 033709 (2013).
- [21] K. Yoshimi, T. Tsumuraya, and T. Misawa, Physical Review Research **3**, 043224 (2021).
- [22] K. Ido, K. Yoshimi, T. Misawa, and M. Imada, npj Quantum Materials **7**, 48 (2022).
- [23] T. Itou, A. Oyamada, S. Maegawa, and R. Kato, Nat. Phys. **6**, 673 (2010).
- [24] M. Yamashita, N. Nakata, Y. Senshu, M. Nagata, H. M. Yamamoto, R. Kato, T. Shibauchi, and Y. Matsuda, Science **328**, 1246 (2010).
- [25] S. Yamashita, T. Yamamoto, Y. Nakazawa, M. Tamura, and R. Kato, Nat. Commun. **2**, 275 (2011).
- [26] D. Watanabe, M. Yamashita, S. Tonegawa, Y. Oshima, H. M. Yamamoto, R. Kato, I. Sheikin, K. Behnia, T. Terashima, S. Uji, T. Shibauchi, and Y. Matsuda, Nat. Commun. **3**, 1090 (2012).
- [27] M. Poirier, M. O. Proulx, and R. Kato, Phys. Rev. B **90**, 045147 (2014).
- [28] T. Yamamoto, T. Fujimoto, T. Naito, Y. Nakazawa,

- M. Tamura, K. Yakushi, Y. Ikemoto, T. Moriwaki, and R. Kato, *Scientific Reports* **7**, 12930 (2017).
- [29] J. M. Ni, B. L. Pan, B. Q. Song, Y. Y. Huang, J. Y. Zeng, Y. J. Yu, E. J. Cheng, L. S. Wang, D. Z. Dai, R. Kato, and S. Y. Li, *Phys. Rev. Lett.* **123**, 247204 (2019).
- [30] P. Bourgeois-Hope, F. Laliberte, E. Lefrancois, G. Grissonnanche, S. R. de Cotret, R. Gordon, S. Kitou, H. Sawa, H. Cui, R. Kato, L. Taillefer, and N. Doiron-Leyraud, *Phys. Rev. X* **9**, 041051 (2019).
- [31] M. Yamashita, *J. Phys. Soc. Jpn.* **88**, 083702 (2019).
- [32] M. Yamashita, Y. Sato, T. Tominaga, Y. Kasahara, S. Kasahara, H. Cui, R. Kato, T. Shibauchi, and Y. Matsuda, *Phys. Rev. B* **101**, 140407(R) (2020).
- [33] T. Nomoto, S. Yamashita, H. Akutsu, Y. Nakazawa, and R. Kato, *Phys. Rev. B* **105**, 245133 (2022).
- [34] K. Ueda, S. Fujiyama, and R. Kato, *Phys. Rev. B* **109**, L140401 (2024).
- [35] O. I. Motrunich, *Phys. Rev. B* **72**, 045105 (2005).
- [36] M. Yamashita, Y. Sato, Y. Kasahara, S. Kasahara, T. Shibauchi, and Y. Matsuda, *Sci. Rep.* **12**, 9187 (2022).
- [37] R. Kato, M. Uebe, S. Fujiyama, and H. B. Cui, *Crystals* **12**, 102 (2022).
- [38] K. Watanabe, H. Kawamura, H. Nakano, and T. Sakai, *J. Phys. Soc. Jpn.* **83**, 034714 (2014).
- [39] T. Shimokawa, K. Watanabe, and H. Kawamura, *Phys. Rev. B* **92**, 134407 (2015).
- [40] M. Abdel-Jawad, N. Tajima, R. Kato, and I. Terasaki, *Phys. Rev. B* **88**, 075139 (2013).
- [41] URL will be inserted by publisher.
- [42] P. W. Anderson, *J. Phys. Soc. Jpn.* **9**, 316 (1954).
- [43] A. Bencini and D. Gatteschi, *Electron paramagnetic resonance of exchange coupled systems* (Springer, Berlin, 1990).
- [44] T. Okuda and M. Date, *J. Phys. Soc. Jpn.* **28**, 308 (1970).
- [45] M. A. Fayzullin, R. M. Eremina, M. V. Eremin, A. Dittl, N. van Well, F. Ritter, W. Assmus, J. Deisenhofer, H.-A. K. von Nidda, and A. Loidl, *Phys. Rev. B* **88**, 174421 (2013).
- [46] M. J. Hennessy, C. D. McElwee, and P. M. Richards, *Phys. Rev. B* **7**, 930 (1973).
- [47] T. T. P. Cheung, Z. G. Soos, R. E. Dietz, and F. R. Merritt, *Phys. Rev. B* **17**, 1266 (1978).
- [48] T. Takahashi, H. Doi, and H. Nagasawa, *J. Phys. Soc. Jpn.* **48**, 423 (1980).
- [49] H. Tanaka, S. I. Kuroda, T. Yamashita, M. Mitsumi, and K. Toriumi, *Phys. Rev. B* **73**, 245102 (2006).
- [50] M. J. Frisch, G. W. Trucks, H. B. Schlegel, G. E. Scuseria, M. A. Robb, J. R. Cheeseman, G. Scalmani, V. Barone, G. A. Petersson, H. Nakatsuji, X. Li, M. Caricato, A. V. Marenich, J. Bloino, B. G. Janesko, R. Gomperts, B. Mennucci, H. P. Hratchian, J. V. Ortiz, A. F. Izmaylov, J. L. Sonnenberg, Williams, F. Ding, F. Lipparini, F. Egidi, J. Goings, B. Peng, A. Petrone, T. Henderson, D. Ranasinghe, V. G. Zakrzewski, J. Gao, N. Rega, G. Zheng, W. Liang, M. Hada, M. Ehara, K. Toyota, R. Fukuda, J. Hasegawa, M. Ishida, T. Nakajima, Y. Honda, O. Kitao, H. Nakai, T. Vreven, K. Throssell, J. A. Montgomery Jr., J. E. Peralta, F. Ogliaro, M. J. Bearpark, J. J. Heyd, E. N. Brothers, K. N. Kudin, V. N. Staroverov, T. A. Keith, R. Kobayashi, J. Normand, K. Raghavachari, A. P. Rendell, J. C. Burant, S. S. Iyengar, J. Tomasi, M. Cossi, J. M. Millam, M. Klene, C. Adamo, R. Cammi, J. W. Ochterski, R. L. Martin, K. Morokuma, O. Farkas, J. B. Foresman, and D. J. Fox, *Gaussian 16 rev. b.01* (2016).
- [51] F. L. Pratt, S. J. Blundell, T. Jestadt, B. W. Lovett, R. M. Macrae, and W. Hayes, *Magn. Reson. Chem.* **38**, S27 (2000).
- [52] K. Momma and F. Izumi, *J. Appl. Crystallogr.* **44**, 1272 (2011).
- [53] T. Misawa, K. Yoshimi, and T. Tsumuraya, *Phys. Rev. Res.* **2**, 032072(R) (2020).
- [54] J. P. Perdew, K. Burke, and M. Ernzerhof, *Phys. Rev. Lett.* **77**, 3865 (1996).
- [55] P. Giannozzi, O. Andreussi, T. Brumme, O. Bunau, M. B. Nardelli, M. Calandra, R. Car, C. Cavazzoni, D. Ceresoli, M. Cococcioni, N. Colonna, I. Carnimeo, A. D. Corso, S. de Gironcoli, P. Delugas, R. A. DiStasio, A. Ferretti, A. Floris, G. Fratesi, G. Fugallo, R. Gebauer, U. Gerstmann, F. Giustino, T. Gorni, J. Jia, M. Kawamura, H.-Y. Ko, A. Kokalj, E. Küçükbenli, M. Lazzeri, M. Marsili, N. Marzari, F. Mauri, N. L. Nguyen, H.-V. Nguyen, A. O. de-la Roza, L. Paulatto, S. Poncé, D. Rocca, R. Sabatini, B. Santra, M. Schlipf, A. P. Seitsonen, A. Smogunov, I. Timrov, T. Thonhauser, P. Umari, N. Vast, X. Wu, and S. Baroni, *Journal of Physics: Condensed Matter* **29**, 465901 (2017).
- [56] D. R. Hamann, *Phys. Rev. B* **88**, 085117 (2013).
- [57] M. Schlipf and F. Gygi, *Computer Physics Communications* **196**, 36 (2015).
- [58] N. Marzari and D. Vanderbilt, *Phys. Rev. B* **56**, 12847 (1997).
- [59] I. Souza, N. Marzari, and D. Vanderbilt, *Phys. Rev. B* **65**, 035109 (2001).
- [60] H. Seo, T. Tsumuraya, M. Tsuchiizu, T. Miyazaki, and R. Kato, *J. Phys. Soc. Jpn.* **84**, 044716 (2015).
- [61] S. Fujiyama and R. Kato, *Phys. Rev. Lett.* **122**, 147204 (2019).
- [62] T. Miyazaki and T. Ohno, *Phys. Rev. B* **68**, 035116 (2003).
- [63] R. Coldea, D. A. Tennant, A. M. Tsvelik, and Z. Tylczynski, *Phys. Rev. Lett.* **86**, 1335 (2001).
- [64] M. Kohno, O. A. Starykh, and L. Balents, *Nat. Phys.* **3**, 790 (2007).
- [65] O. A. Starykh and L. Balents, *Phys. Rev. Lett.* **98**, 077205 (2007).
- [66] Y. Hayashi and M. Ogata, *J. Phys. Soc. Jpn.* **76**, 053705 (2007).
- [67] S. Yunoki and S. Sorella, *Phys. Rev. B* **74**, 014408 (2006).